Title: Population clustering of structural brain aging and its association with brain development

Authors: Haojing Duan[1,2], Runye Shi[3], Jujiao Kang[1,2], Tobias Banaschewski[4], Arun L. W. Bokde[5], Christian Büchel[6], Sylvane Desrivières[7], Herta Flor[8,9], Antoine Grigis[10], Hugh Garavan[11], Penny A. Gowland[12], Andreas Heinz[13], Rüdiger Brühl[14], Jean-Luc Martinot[15,16], Marie-Laure Paillère Martinot[15,17], Eric Artiges[15,16], Frauke Nees[4,8,18], Dimitri Papadopoulos Orfanos[10], Luise Poustka[19], Sarah Hohmann[4], Nathalie Holz[4], Juliane H. Fröhner[20], Michael N. Smolka[20], Nilakshi Vaidya[21], Henrik Walter[13], Robert Whelan[22], Gunter Schumann[1,21,23,24], Xiaolei Lin[3,25*], Jianfeng Feng[1,2,3,26.27,28*], IMAGEN consortium

Affiliations:

[1] Institute of Science and Technology for Brain-Inspired Intelligence, Fudan University, Shanghai, China

[2] Key Laboratory of Computational Neuroscience and Brain-Inspired Intelligence (Fudan University), Ministry of Education, China

[3] School of Data Science, Fudan University, Shanghai, China

[4] Department of Child and Adolescent Psychiatry and Psychotherapy, Central Institute of Mental Health, Medical Faculty Mannheim, Heidelberg University, Square J5, 68159 Mannheim, Germany

[5] Discipline of Psychiatry, School of Medicine and Trinity College Institute of Neuroscience, Trinity College Dublin, Dublin, Ireland

[6] University Medical Centre Hamburg-Eppendorf, Hamburg, Germany

[7] Social Genetic and Developmental Psychiatry Centre, Institute of Psychiatry, Psychology and Neuroscience, King's College London, London, UK

[8] Institute of Cognitive and Clinical Neuroscience, Central Institute of Mental Health, Medical Faculty Mannheim, Heidelberg University, Square J5, Mannheim, Germany

[9] Department of Psychology, School of Social Sciences, University of Mannheim, 68131 Mannheim, Germany

[10] NeuroSpin, CEA, Université Paris-Saclay, F-91191 Gif-sur-Yvette, France

[11] Departments of Psychiatry and Psychology, University of Vermont, 05405 Burlington, Vermont, USA

[12] Sir Peter Mansfield Imaging Centre School of Physics and Astronomy, University of Nottingham, University Park, Nottingham, United Kingdom

[13] Department of Psychiatry and Psychotherapy CCM, Charité – Universitätsmedizin Berlin, corporate member of Freie Universität Berlin, Humboldt-Universität zu Berlin, and Berlin Institute of Health, Berlin, Germany

[14] Physikalisch-Technische Bundesanstalt (PTB), Braunschweig and Berlin, Germany

[15] Institut National de la Santé et de la Recherche Médicale, INSERM U1299 "Developmental Trajectories and Psychiatry", Université Paris-Saclay, Ecole Normale supérieure Paris-Saclay, CNRS, Centre Borelli, Gif-sur-Yvette, France

[16] Psychiatry Department, EPS Barthélémy Durand, Etampes; France

[17] AP-HP. Sorbonne Université, Department of Child and Adolescent Psychiatry, Pitié-Salpêtrière Hospital, Paris, France

[18] Institute of Medical Psychology and Medical Sociology, University Medical Center Schleswig-Holstein Kiel University, Kiel, Germany

[19] Department of Child and Adolescent Psychiatry and Psychotherapy, University Medical Centre

Göttingen, von-Siebold-Str. 5, 37075, Göttingen, Germany
[20] Department of Psychiatry and Neuroimaging Center, Technische Universität Dresden, Dresden, Germany
[21] Department of Psychiatry and Neurosciences, Charité–Universitätsmedizin Berlin, corporate member of Freie Universität BerlinHumboldt-Universität zu Berlin, and Berlin Institute of Health, Berlin, Germany
[22] School of Psychology and Global Brain Health Institute, Trinity College Dublin, Ireland
[23] Centre for Population Neuroscience and Stratified Medicine (PONS Centre), ISTBI, Fudan University, Shanghai, China
[24] Centre for Population Neuroscience and Stratified Medicine (PONS), Department of Psychiatry and Psychotherapy, Charité Universitätsmedizin Berlin, Germany
[25] Huashan Institute of Medicine, Huashan Hospital affiliated to Fudan University, Shanghai, China
[26] MOE Frontiers Center for Brain Science, Fudan University, Shanghai, China
[27] Zhangjiang Fudan International Innovation Center, Shanghai, China
[28] Department of Computer Science, University of Warwick, Coventry CV4 7AL, UK

* Correspondence authors.
Xiaolei Lin (Address: School of Data Science, Fudan University, Shanghai, 200433, China. Email: xiaoleilin@fudan.edu.cn)
or
Jianfeng Feng (Address: Institute of Science and Technology for Brain-inspired Intelligence, Fudan University, Shanghai, 200433, China. Email: jianfeng64@gmail.com)

Abstract

Structural brain aging has demonstrated strong inter-individual heterogeneity and mirroring patterns with brain development. However, due to the lack of large-scale longitudinal neuroimaging studies, most of the existing research focused on the cross-sectional changes of brain aging. In this investigation, we present a data-driven approach that incorporate both cross-sectional changes and longitudinal trajectories of structural brain aging and identified two brain aging patterns among 37,013 healthy participants from UK Biobank. Participants with accelerated brain aging also demonstrated accelerated biological aging, cognitive decline and increased genetic susceptibilities to major neuropsychiatric disorders. Further, by integrating longitudinal neuroimaging studies from a multi-center adolescent cohort, we validated the "last in, first out" mirroring hypothesis and identified brain regions with manifested mirroring patterns between brain aging and brain development. Genomic analyses revealed risk loci and genes contributing to accelerated brain aging and delayed brain development, providing molecular basis for elucidating the biological mechanisms underlying brain aging and related disorders.

Introduction

The structure of the brain undergoes continual changes throughout the entire lifespan, with structural brain alterations intimately linking brain development and brain aging[1,2]. Brain aging is a progressive process that often co-occurs with biological aging and declines of cognitive functions[3–5], which contribute to the onset and acceleration of neurodegenerative[6] and neuropsychiatric disorders[7]. Studies on healthy brain aging have revealed significant inter-individual heterogeneity in the patterns of neuroanatomical changes[8,9]. Therefore, examining the patterns of structural brain aging and its associations with cognitive decline is of paramount importance in understanding the diverse biological mechanisms of age-related neuropsychiatric disorders.

Despite the fact that there exist large differences between brain development and brain aging[10], a discernible association between these two processes remains evident. Direct comparisons of brain development and brain aging using structural MRI indicated a “last in, first out” mirroring pattern, where brain regions develop relatively late during adolescence demonstrated accelerated degeneration in older ages[11,12]. In addition, brain regions with strong mirroring effects showed increased vulnerability to neurodegenerative and neuropsychiatric disorders, including Alzheimer’s disease and schizophrenia[13]. However, due to the lack of large-scale longitudinal MRI studies during adolescence and mid-to-late adulthood, validation of the “last in, first out” mirroring hypothesis remains unavailable.

Prior investigations have largely focused on regional and cross-sectional changes of brain aging[9,13,14], with relatively few studies exploring longitudinal trajectories of brain aging and its associations with brain development[8,15,16]. In this article, we present a data-driven approach to examine the population clustering of longitudinal brain aging trajectories using structure MRI data obtained from 37,013 healthy individuals during mid-to-late adulthood (44-82 years), and explore its association with biological aging, cognitive decline and susceptibilities for neuropsychiatric disorders. Further, mirroring patterns between longitudinal brain development and brain aging are investigated by comparing the region-specific aging / developmental trajectories, and manifestation of the mirroring patterns are investigated across the whole-brain and among participants with different brain aging patterns. Genomic analyses

are conducted to reveal risk loci and genes associated with accelerated brain aging and delayed brain development.

Results

Longitudinal trajectories of whole-brain gray matter volume in mid-to-late adulthood define two brain aging patterns.

Figure 1 provides the data sources, analytical workflow and research methodology of this study. After the sample selection process (Appendix 1—figure 1, Appendix 1—tables 1 and 2), longitudinal grey matter volume (GMV) trajectories in 40 ROIs (33 cortical and 7 subcortical ROIs, see Appendix 1—table 3) were estimated for each of the 37,013 healthy participants in UK Biobank. The first 15 principal components derived from dimensionality reduction via principal component analysis were used in the clustering analysis (see Methods)[17,18]. Two brain aging patterns were identified, where 18,929 (51.1%) participants with the first brain aging pattern (pattern 1) had higher total GMV at baseline and a slower rate of GMV decrease over time, and the remaining participants with the second pattern (pattern 2) had lower total GMV at baseline and a faster rate of GMV decrease (Figure 2a). Comparing the region-specific rate of GMV decrease, pattern 2 showed a more rapid GMV decrease in medial occipital (lingual gyrus, cuneus and pericalcarine cortex) and medial temporal (entorhinal cortex, parahippocampal gyrus) regions (Figure 2b, c and Appendix 1—figure 2), which had the largest loadings in the second and third principal components (Appendix 1—table 4). These two patterns can be clearly stratified by both linear and non-linear dimensionality reduction methods, indicating distinct structural differences in brain aging between patterns (Appendix 1—figure 3). Sample characteristics of these 37,013 UK Biobank participants stratified by brain aging patterns are summarized in Appendix 1—table 5. Overall, participants with different brain aging patterns had similar distributions with regard to age, sex, ethnicity, smoking status, Townsend deprivation index (TDI), body mass index (BMI) and years of schooling.

Brain aging patterns were significantly associated with biological aging.

To explore the relationships between structural brain aging and biological aging, we investigated the distribution of aging biomarkers, such as telomere length and PhenoAge[19], across brain aging patterns identified above (Figure 3 and Appendix 1—table 6). Compared to pattern 1, participants in pattern 2 with more rapid GMV decrease had shorter leucocyte telomere length ($P = 0.009$, Cohen's $D = -0.028$) and this association remained consistent after adjusting for sex, age, ethnic, BMI, smoking status and alcohol intake frequency[20]. Next, we examined PhenoAge, which was developed as an aging biomarker incorporating composite clinical and biochemical data[19], and observed higher PhenoAge among participants with brain aging pattern 2 compared to pattern 1 ($P = 0.019$, Cohen's $D = 0.027$). Again, the association remained significant after adjusting for sex, age, ethnic, BMI, smoking status, alcohol intake frequency and education years ($P = 3.05 \times 10^{-15}$, Cohen's $D = 0.092$). Group differences in terms of each individual component of PhenoAge (including albumin, creatinine, glucose, c-reactive protein, lymphocytes percentage, mean corpuscular volume, erythocyte distribution width, alkaline phosphatase and leukocyte count) were also investigated and results were consistent with PhenoAge (Appendix 1—figure 4).

Accelerated brain aging was associated with cognitive decline and increased genetic susceptibilities to attention-deficit/hyperactivity disorder and delayed brain development. Next, we conducted comprehensive comparisons of cognitive functions between participants with different brain aging patterns. In general, those with brain aging pattern 2 (lower baseline total GMV and more rapid GMV decrease) exhibited worse cognitive performances compared to pattern 1. Specifically, brain aging pattern 2 showed lower numbers of correct pairs matching ($P = 0.006$, Cohen's $D = -0.029$), worse prospective memory (OR = 0.943, 95% CI [0.891, 0.999]), lower fluid intelligence ($P < 1.00 \times 10^{-20}$, Cohen's $D = -0.102$), and worse numeric memory ($P = 5.97 \times 10^{-11}$, Cohen's $D = -0.082$). No statistically significant differences were observed in terms of the reaction time ($P = 0.99$) and prospective memory ($P = 0.052$) between these two brain aging patterns after FDR correction. Results were consistent when using models adjusted for sex, age, and socioeconomic status (TDI, education and income)[21,22]

(Figure 4). Full results demonstrating the associations between brain aging patterns and cognitive functions are presented in Appendix 1—table 7.

Having observed cognitive decline among participants with accelerated brain aging pattern, we next investigated whether brain aging patterns were associated with genetic vulnerability to major neuropsychiatric disorders. Since current GWAS are under-powered for attention-deficit/hyperactivity disorder (ADHD) and autism spectrum disorders (ASD) and the difficulty in identifying genetic variants was likely due to their polygenic nature, we calculated the corresponding polygenic risk scores (PRS) using multiple p value thresholds. This approach enabled robust investigation of the association between genetic susceptibility of neuropsychiatric disorders and brain imaging phenotypes. PRS for major neuro-developmental disorders including attention-deficit/hyperactivity disorder (ADHD) and autism spectrum disorders (ASD), neurodegenerative diseases including Alzheimer's disease (AD) and Parkinson's disease (PD), neuropsychiatric disorders including bipolar disorder (BIP), major depressive disorder (MDD), and schizophrenia (SCZ), and delayed structural brain development (GWAS from an unpublished longitudinal neuroimaging study)[23] were calculated for each participant using multiple P value thresholds (from 0.005 to 0.5 at intervals of 0.005) and results were then averaged over all thresholds (Figure 5). The primary GWAS datasets used for calculating the PRS were listed in Appendix 1—table 8. Overall, we observed increased genetic susceptibility to ADHD ($P = 0.040$) and delayed brain development ($P = 1.48 \times 10^{-6}$) among participants with brain aging pattern 2 after FDR correction, while no statistically significant differences were observed for ASD, AD, PD, BIP, MDD and SCZ (Figure 5). Details regarding the genetic liability to other common diseases and phenotypes using enhanced PRS from UK Biobank are displayed in Appendix 1—tables 9 and 10.

Genome Wide Association Studies (GWAS) identified significant genetic loci associated with accelerated brain aging.

Having observed significant associations between brain aging patterns and cognitive performances / genetic liabilities to major neurodevelopmental disorders, we further investigated if there exist genetic variants contributing to individualized brain aging phenotype.

We conducted genome-wide association studies (GWAS) using estimated total GMV at 60 years old as the phenotype. This phenotype was derived by adding individual specific deviations to the population averaged total GMV, thus providing additional information compared to studies using only cross-sectional neuroimaging phenotypes.

Six independent single nucleotide polymorphisms (SNPs) were identified at genome-wide significance level ($P < 5 \times 10^{-8}$) (Figure 6) and were subsequently mapped to genes using NCBI, Ensembl and UCSC Genome Browser database (Appendix 1—table 11). Among them, two SNPs (rs10835187 and rs779233904) were also found to be associated with multiple brain imaging phenotypes in previous studies[24], such as regional and tissue volume, cortical area and white matter tract measurements. Compared to the GWAS using global gray matter volume as the phenotype, our GWAS revealed additional signal in chromosome 7 (rs7776725), which was mapped to the intron of FAM3C and encodes a secreted protein involved in pancreatic cancer[25] and Alzheimer's disease[26]. This signal was further validated to be associated with specific brain aging mode by another study using a data-driven decomposition approach[27]. In addition, another significant loci (rs10835187, $P = 1.11 \times 10^{-13}$) is an intergenic variant between gene LGR4-AS1 and LIN7C, and was reported to be associated with bone density and brain volume measurement[24,28]. *LIN7C* encodes the Lin-7C protein, which is involved in the localization and stabilization of ion channels in polarized cells, such as neurons and epithelial cells[29,30]. Previous study has revealed the association of both allelic and haplotypic variations in the *LIN7C* gene with ADHD[31].

Mirroring patterns between brain aging and brain development.

Having observed significant associations between brain aging and genetic susceptibility to neurodevelopmental disorders, we are now interested in examining the mirroring patterns between brain aging and brain development in the whole population, and whether these mirroring patterns were more pronounced in those with accelerated brain aging. Adolescents in the IMAGEN cohort showed more rapid GMV decrease in the frontal and parietal lobes, especially the frontal pole, superior frontal gyrus, rostral middle frontal gyrus, inferior parietal lobule and superior parietal lobule, while those in their mid-to-late adulthood showed more

accelerated GMV decrease in the temporal lobe, including medial orbitofrontal cortex, inferior parietal lobule and lateral occipital sulcus (Figure 7a). The mirroring patterns (with slower GMV decrease during brain development and more rapid GMV decrease during brain aging) were particularly prominent in inferior temporal gyrus, caudal anterior cingulate cortex, fusiform cortex, middle temporal gyrus and rostral anterior cingulate cortex (Figure 7b). The regional mirroring patterns became weaker when we focus on late brain aging at age 75 years old, especially in the frontal lobe and cingulate cortex. Further, mirroring patterns were represented more prominently in participants with brain aging pattern 2, where stronger mirroring between brain aging and brain development was observed in frontotemporal area, including lateral occipital sulcus and lingual gyrus (Figure 7c).

Gene expression profiles were associated with delayed brain development and accelerated brain aging.

The Allen Human Brain Atlas (AHBA) transcriptomic dataset (http://human.brain-map.org) were used to obtain the spatial correlation between gene expression profiles across cortex and structural brain development/aging via partial least square (PLS) regression. The first PLS component explained 24.7% and 53.6% of the GMV change during brain development (estimated at age 15y, $r_{spearman} = 0.51$, $P_{permutation} = 0.03$) and brain aging (estimated at age 55y, $r_{spearman} = 0.49$, $P_{permutation} = 1.5 \times 10^{-4}$), respectively. Seventeen of the 45 genes mapped to GWAS significant SNP were found in AHBA, with *LGR4* ($r_{spearman} = 0.56$, $P_{permutation} < 0.001$) significantly associated with delayed brain development and *ESR1* ($r_{spearman} = 0.53$, $P_{permutation} < 0.001$) and *FAM3C* ($r_{spearman} = -0.37$, $P_{permutation} = 0.004$) significantly associated with accelerated brain aging. *BDNF-AS* was positively associated with both delayed brain development and accelerated brain aging after spatial permutation test (Appendix 1—tables 12 and 13).

Next, we screened the genes based on their contributions and effect directions to the first PLS components in brain development and brain aging. 990 and 2293 genes were identified to be positively associated with brain development and negatively associated with brain aging at FDR corrected P value of 0.005, respectively, representing gene expressions associated with

delayed brain development and accelerated brain aging. These genes were then tested for enrichment of GO biological processes and KEGG pathways. Genes associated with delayed brain development showed significant enrichment in "regulation of trans-synaptic signaling", "forebrain development", "signal release" and "cAMP signaling pathway" (Figure 8a), and genes associated with accelerated brain aging showed significant enrichment in "macroautophagy", "establishment of protein localization to organelle", "histone modification", and "pathways of neurodegeneration – multiple diseases" (Figure 8b). Full results of the gene set enrichment analysis were provided in Appendix 1—figure 5. In summary, the analyses from using the databases of GO biological processes and KEGG Pathways indicate synaptic transmission as an important process in the common mechanisms of brain development and aging, and cellular processes (autophagy), as well as the progression of neurodegenerative diseases, are important processes in the mechanisms of brain aging.

Discussion

In this study, we adopted a data-driven approach and revealed two distinct brain aging patterns using large-scale longitudinal neuroimaging data in mid-to-late adulthood. Compared to brain aging pattern 1, brain aging pattern 2 were characterized by a faster rate of GMV decrease, accelerated biological aging, cognitive decline, and genetic susceptibility to neurodevelopmental disorders. By integrating longitudinal neuroimaging data from adult and adolescent cohorts, we demonstrated the "last in, first out" mirroring patterns between structural brain aging and brain development, and showed that the mirroring pattern was manifested in the temporal lobe and among participants with accelerated brain aging. Further, genome-wide association studies identified significant genetic loci contributing to accelerated brain aging, while spatial correlation between whole-brain transcriptomic profiles and structural brain aging / development revealed important gene sets associated with both accelerated brain aging and delayed brain development.

Brain aging is closely related to the onset and progression of neurodegenerative and neuropsychiatric disorders. Both neurodegenerative and neuropsychiatric disorders demonstrate strong inter-individual heterogeneity, which prevents the comprehensive

understanding of their neuropathology and neurogenetic basis. Therefore, multidimensional investigation into disease subtyping and population clustering of structural brain aging are crucial in elucidating the sources of heterogeneity and neurophysiological basis related to the disease spectrum[32]. In the last decades, major developments in the subtyping of Alzheimer's disease, dementia and Parkinson's disease, have provided new perspectives regarding their clinical diagnosis, treatment, disease progression and prognostics[32–34]. While previous studies of brain aging mostly focused on the cross-sectional differences between cases and healthy controls, we here delineated the structural brain aging patterns among healthy participants using a novel data-driven approach that captured both cross-sectional and longitudinal trajectories of the whole-brain gray matter volume[35,36]. The two brain aging patterns identified using the above approach showed large differences in the rate of change in medial occipitotemporal gyrus, which is involved in vision, word processing and scene recognition[37–39]. Significant reduction of the gray matter volume and abnormal changes of the functional connectivity in this region were found in subjects with mild cognitive impairment (MCI) and AD, respectively[40,41]. Previous research on brainAGE[3,42] (the difference between chronological age and the age predicted by the machine learning model of brain imaging data) showed that as a biomarker of accelerated brain aging, people with older brainAGE have accelerated biological aging and early signs of cognitive decline, which is consistent with our discoveries in this study. Our results support the establishment of a network connecting brain aging patterns with biological aging profiles involving multi-organ systems throughout the body[43]. Since structural brain patterns might manifest and diverge decades before cognitive decline[44], subtyping of brain aging patterns could aid in the early prediction of cognitive decline and severe neurodegenerative and neuropsychiatric disorders.

Mirroring pattern between brain development and brain aging has long been hypothesized by postulating that phylogenetically newer and ontogenetically less precocious brain structures degenerate relatively early[13]. Early studies have reported a positive correlation between age-related differences of cortical volumes and precedence of myelination of intracortical fibers[45]. Large differences in the patterns of change between adolescent late development and aging in the medial temporal cortex were previously found in studies of brain development and aging

patterns[12]. Here, we compared the annual volume change of the whole-brain gray matter during brain development and early / late stages of brain aging, and found that mirroring patterns are predominantly localized to the lateral / medial temporal cortex and the cingulate cortex. These cortical regions characterized by "last-in, first-out" mirroring patterns showed increased vulnerability to the several neuropsychiatric disorders. For example, regional deficits in the superior temporal gyrus and medial temporal lobe were observed in schizophrenia[46], along with morphological abnormalities in the medial occipitotemporal gyrus[47]. Children diagnosed with ADHD had lower brain surface area in the frontal, cingulate, and temporal regions[48]. Douaud et al.[13] revealed a population transmodal network with lifespan trajectories characterized by the mirroring pattern of development and aging. We investigated the genetic susceptibility to individual-level mirroring patterns based on the lasting impact of neurodevelopmental genetic factors on brain[15], demonstrating that those with more rapidly brain aging patterns have a higher risk of delayed development.

Identifying genes contributing to structural brain aging remains a critical step in understanding the molecular changes and biological mechanisms that govern age-related cognitive decline. Several genetic loci have been reported to be associated with brain aging modes and neurocognitive decline, many of which demonstrated global overlap with neuropsychiatric disorders and their related risk factors[27,49,50]. Here, we focused on the individual brain aging phenotype by estimating individual deviation from the population averaged total GMV and conducted genome-wide association analysis with this phenotype. Our approach identified 6 risk SNPs associated with accelerated brain aging, most of which could be further validated by previous studies using population averaged brain aging phenotypes. However, our approach revealed additional genetic signals and demonstrated genetic architecture underlying brain aging patterns overlap with bone density[28,51]. In addition, molecular profiling of the aging brain has been thoroughly investigated among patients with neurogenerative diseases, but rarely conducted to shed light on the mirroring patterns among healthy participants. Analysis of the spatial correlation between gene expression profiles and structural brain development / aging further identified genes contributing to delayed brain development and accelerated brain aging. Specifically, expression of gene *BDNF-AS* was

significantly associated with both processes. *BDNF-AS* is an antisense RNA gene and plays a role in the pathoetiology of non-neoplastic conditions mainly through the mediation of *BDNF*[52]. LGR4 (associated with delayed brain development) and FAM3C (associated with accelerated brain aging) identified in the spatial genetic association analysis also validated our findings in the GWAS.

There are several limitations in the current study that need to be addressed in future research. Firstly, the UK Biobank cohort, which we leveraged to identify population clustering of brain aging patterns, had a limited number of repeated structural MRI scans. Therefore, it remains challenging to obtain robust estimation of the longitudinal whole-brain GMV trajectory at the individual level. As a robustness check, we have calculated both intra-class correlation and variance of both random intercept and age slope to ensure appropriateness of the mixed effect models. Secondly, although aging is driven by numerous hallmarks, we have only investigated the association between brain aging patterns and biological aging in terms of telomere length and blood biochemical markers due to limitations of data access. Other dimensions of aging hallmarks and their relationship with structural brain aging need to be investigated in the future. Thirdly, our genomic analyses were restricted to "white British" participants of European ancestry. The diversity of genomic analyses will continue to improve as the sample sizes of GWAS of non-European ancestry increase. Further, although the gene expression maps from Allen Human Brain Atlas enabled us to gain insights into the spatial coupling between gene expression profiles and mirroring patterns of the brain, the strong inter-individual variation of whole-brain gene expression levels and large temporal span of the human brain samples may lead to the inaccurate correspondence in the observed associations. Finally, we focused on structural MRIs in deriving brain aging patterns in this analysis, future investigations could consider other brain imaging modalities from a multi-dimensional perspective. Nevertheless, our study represents a novel attempt for population clustering of structural brain aging and validated the mirroring pattern hypothesis by leveraging large-scale adolescent and adult cohorts.

Methods

Participants T1-weighted brain MRI images were obtained from 37,013 individuals aged 44-82 years old from UK Biobank (36,914 participants at baseline visit in 2014+, 4,007 participants at the first follow-up visit in 2019+). All participants from UK Biobank provided written informed consent, and ethical approval was granted by the North West Multi-Center Ethics committee (https://www.ukbiobank.ac.uk/learn-more-about-uk-biobank/about-us/ethics) with research ethics committee (REC) approval number 16/NW/0274. Participants were excluded if they were diagnosed with severe psychiatric disorders or neurological diseases using ICD-10 primary and secondary diagnostic codes or from self-reported medical conditions at UK Biobank assessment center (see Appendix 1—tables 1 and 2). Data were obtained under application number 19542. 1,529 adolescents with structural MRI images were drawn from the longitudinal project IMAGEN (1,463 at age 14, 1,377 at age 19 and 1,148 at age 23), of which the average number of MRI scans was 2.61 per adolescent. The lMAGEN study was approved by local ethics research committees of King's College London, University of Nottingham. Trinity College Dublin, University of Heidelberg, Technische Universität Dresden, Commissariat à l'Énergie Atomique et aux Énergies Alternatives, and University Medical Center at the University of Hamburg in compliance with the Declaration of Helsinki[53]. Informed consent was given by all participants and a parent/guardian of each participant.

MRI acquisition Quality-controlled T1-weighted neuroimaging data from UK Biobank and IMAGEN were processed using FreeSurfer v6.0. Detailed imaging processing pipeline can be found online for UK Biobank (https://biobank.ctsu.ox.ac.uk/crystal/crystal/docs/brain_mri.pdf) and IMAGEN (https://github.com/imagen2/imagen_mri). Briefly, cortical gray matter volume (GMV) from 33 regions in each hemisphere were generated using Desikan–Killiany Atlas[54], and total gray matter volume (TGMV), intracranial volume (ICV) and subcortical volume were derived from ASEG atlas[55] (See Appendix 1—table 3). Regional volume was averaged across left and right hemispheres. To avoid deficient segmentation or parcellation, participants with TGMV, ICV or regional GMV beyond 4 standard deviations from the sample mean were considered as outliers and removed from the following analyses.

Identification of longitudinal brain aging patterns Whole-brain GMV trajectory was estimated for each participant in 40 brain regions of interest (ROIs) (33 cortical regions and 7 subcortical regions), using mixed effect regression model with fixed linear and quadratic age effects, random intercept and random age slope. Covariates include sex, assessment center, handedness, ethnic, and ICV. Models with random intercept and with both random intercept and random age slope were compared using AIC, BIC and evaluation of intra-class correlation (ICC). Results suggested that random age slope model should be chosen for almost all ROIs (Appendix 1—table 14). Deviation of regional GMV from the population average was calculated for each participant at age 60 years and dimensionality reduction was conducted via principal component analysis (PCA). The first 15 principal components explaining approximately 70% of the total variations of regional GMV deviation were used in multivariate k-means clustering. Optimal number of clusters was chosen using both elbow diagram and contour coefficient (Appendix 1—figure 6). Rates of volumetric change for total gray matter and each ROI were estimated using generalized additive mixed effect models (GAMM) with fixed cubic splines of age, random intercept and random age slope, which incorporates both cross-sectional between-subject variation and longitudinal within-subject variation from 40,921 observations and 37,013 participants. Covariates include sex, assessment center, handedness, ethnic, and ICV. We also applied PCA and locally linear embedding (LLE)[56] to the adjusted GMV ROIs in order to map the high-dimensional imaging-derived phenotypes to a low-dimensional space for stratification visualisation. The GMV of 40 ROIs at baseline were linearly adjusted for sex, assessment center, handedness, ethnic, ICV, and second-degree polynomial in age to be consistent with the whole-brain GMV trajectory model.

Association between brain aging patterns and biological aging, cognitive decline and genetic susceptibilities of neuropsychiatric disorders Individuals with Z-standardized leucocyte telomere length[57] and blood biochemistry (which were used to calculate PhenoAge[19] that characterizes biological aging) outside 4 standard deviations from the sample mean were excluded for better quality control. A total of 11 cognitive tests performed on the touchscreen

questionnaire were included in the analysis. More information about the cognitive tests is provided in Supplementary Information. Comparisons of biological aging (leucocyte telomere length, PhenoAge) and cognitive function were conducted among participants with different brain aging patterns using both unadjusted and adjusted multivariate regression models with Bonferroni / FDR correction. Polygenic Risk Scores (PRS) were calculated for autism spectrum disorder (ASD), attention deficit hyperactivity disorder (ADHD), Alzheimer's disease (AD), Parkinson's Disease (PD), bipolar disorder (BIP), major depressive disorder (MDD), schizophrenia (SCZ) and delayed brain development using GWAS summary statistics[23] at multiple P value thresholds (from 0.005 to 0.5 at intervals of 0.005, and 1), with higher P value thresholds incorporating larger number of independent SNPs. After quality control of genotype and imaging data, PRSs were generated for 25,861 participants on UK Biobank genotyping data. SNPs were pruned and clumped with a cutoff $r^2 \geq 0.1$ within a 250 kb window. All calculations were conducted using PRSice v2.3.5[58]. Enhanced PRS from UK Biobank Genomics for multiple diseases were also tested. Detailed instructions for calculating enhanced PRS in UK Biobank can be found in research of Thompson et al.[59] Comparisons of neuropsychiatric disorders were conducted among participants with different brain aging patterns using t test with FDR correction. All statistical tests were two-sided.

Genome Wide Association Study to identify SNPs associated with brain aging patterns

We performed Genome-wide association studies (GWAS) on individual deviations of total GMV relative to the population average at 60 years using PLINK 2.0[60]. Variants with missing call rates exceeding 5%, minor allele frequency below 0.5% and imputation INFO score less than 0.8 were filtered out after the genotyping quality control for UK Biobank Imputation V3 dataset. Among the 337,138 unrelated "white British" participants of European ancestry included in our study, 25,861 with recent UK ancestry and accepted genotyping and imaging quality control were included in the GWAS. The analyses were further adjusted for age, age2, sex, assessment center, handedness, ethnic, ICV, and the first 10 genetic principal components. Genome-wide significant SNPs ($P < 5\times10^{-8}$) obtained from the GWAS were clumped by linkage disequilibrium (LD) ($r^2 < 0.1$ within a 250 kb window) using UKB release2b White

454 British as the reference panel. We subsequently performed gene-based annotation in FUMA[61]
455 using genome-wide significant SNPs and SNPs in close LD ($r^2 \geq 0.1$) using Annotate Variation
456 (ANNOVAR) on Ensemble v102 genes[62].
457
458 **Mirroring patterns between brain aging and brain development** To validate the "last in,
459 first out" mirroring hypothesis, we evaluated the structural association between brain
460 development and brain aging. Longitudinal neuroimaging data from 1,529 adolescents in the
461 IMGAEN cohort and 3,908 mid-to-late adulthood in the UK Biobank cohort were analyzed.
462 Annual percentage volume change (APC) for each ROI was calculated among individuals with
463 at least 2 structural MRI scans by subtracting the baseline GMV from follow-up GMV and
464 dividing by the number of years between baseline and follow-up visits. Region-specific APC
465 was regressed on age using smoothing spline with cross validated degree of freedom. Estimated
466 APC for each ROI was obtained at age 15y for adolescents and at age 55y (early aging) and
467 75y (late aging) for participants in UK Biobank. Region-specific APC during adolescence (or
468 mid-to-late adulthood) was then standardized across all cortical regions to create the brain
469 development (or aging) map. Finally, the brain development map and brain aging map were
470 compared to assess the mirroring pattern for each ROI in the overall population and across
471 different aging subgroups.
472
473 **Gene Expression Analysis** The Allen Human Brain Atlas (AHBA) dataset
474 (http://human.brain-map.org), which comprises gene expression measurements in six
475 postmortem adults (age 24–57y) across 83 parcellated brain regions[63,64], were used to identify
476 gene expressions significantly associated with structural brain development and aging. The
477 expression profiles of 15,633 genes were averaged across donors to form a $83 \times 15{,}633$
478 transcriptional matrix and partial least squares (PLS) regression was adopted for analyzing the
479 association between regional change rate of gray matter volume and gene expression profiles.
480 Specifically, estimated regional APC at 15 (obtained from IMAGEN cohort) and 55 years old
481 (obtained from UK Biobank) were regressed on the high-dimensional gene expression profiles
482 upon regularization. Associations between the first PLS component and estimated APC during

brain development and brain aging were tested by spatial permutation analysis (10,000 times)[65]. Additionally, gene expression profiles of genes mapped to GWAS significant SNP were extracted from AHBA. The association between gene expression profiles of mapped genes and estimated APC during brain development and aging was also tested by spatial permutation analysis. Statistical significance of each gene's contribution to the first PLS component was tested with standard error calculated using bootstrap[66–68], and genes significantly associated with delayed brain development and accelerated brain aging were selected. Enrichment of Kyoto Encyclopedia of Genes and Genomes (KEGG) pathways and gene ontology (GO) of biological processes for these selected genes were analyzed using R package clusterProfiler[69]. All statistical significances were corrected for multiple testing using FDR.

Data availability

The summary statistics of GWAS for individual deviations of total GMV is available at link. All the UK Biobank data used in the study are available at https://www.ukbiobank.ac.uk. The IMAGEN project data are available at https://imagen-project.org. GWAS summary statistics used to calculate the PRS are available in the Appendix 1—table 8. Human gene expression data are available in the Allen Human Brain Atlas dataset: https://human.brainmap.org.

Code availability

R version 4.2.0 was used to perform statistical analyses. FreeSurfer version 6.0 was used to process neuroimaging data. lme4 1.1 in R version 4.2.0 was used to perform longitudinal data analyses. PRSice version 2.3.5 (https://choishingwan.github.io/PRSice/) was used to calculate the PRS. PLINK 2.0 (www.cog-genomics.org/plink/2.0/) and FUMA version 1.5.6 (https://fuma.ctglab.nl/) were used to perform genome-wide association analysis, and ANNOVAR was used to perform gene-based annotation. AHBA microarray expression data were processed using abagen toolbox version 0.1.3 (https://doi.org/10.5281/zenodo.5129257). The rotate_parcellation code used to perform a spatial permutation test of a parcellated cortical map: https://github.com/frantisekvasa/rotate_parcellation. Code for PLS analysis and bootstrapping to estimate PLS weights are available at https://github.com/KirstieJane/NSPN_WhitakerVertes_PNAS2016/tree/master/SCRIPTS. clusterProfiler 4.6 in R version 4.2.0 was used to analyze gene-set enrichment.

References

1. Fjell, A. M. & Walhovd, K. B. Structural brain changes in aging: courses, causes and cognitive consequences. *Reviews in the Neurosciences* **21**, 187–222 (2010).
2. Shaw, P. *et al.* Neurodevelopmental trajectories of the human cerebral cortex. *Journal of neuroscience* **28**, 3586–3594 (2008).
3. Elliott, M. L. *et al.* Brain-age in midlife is associated with accelerated biological aging and cognitive decline in a longitudinal birth cohort. *Molecular psychiatry* **26**, 3829–3838 (2021).
4. Mattson, M. P. & Arumugam, T. V. Hallmarks of brain aging: adaptive and pathological modification by metabolic states. *Cell metabolism* **27**, 1176–1199 (2018).
5. Park, D. C. & Reuter-Lorenz, P. The adaptive brain: aging and neurocognitive scaffolding. *Annual review of psychology* **60**, 173–196 (2009).
6. Mariani, E., Polidori, M., Cherubini, A. & Mecocci, P. Oxidative stress in brain aging, neurodegenerative and vascular diseases: an overview. *Journal of Chromatography B* **827**, 65–75 (2005).
7. Kaufmann, T. *et al.* Common brain disorders are associated with heritable patterns of apparent aging of the brain. *Nature neuroscience* **22**, 1617–1623 (2019).
8. Raz, N., Ghisletta, P., Rodrigue, K. M., Kennedy, K. M. & Lindenberger, U. Trajectories of brain aging in middle-aged and older adults: regional and individual differences. *Neuroimage* **51**, 501–511 (2010).
9. Raz, N. & Rodrigue, K. M. Differential aging of the brain: patterns, cognitive correlates and modifiers. *Neuroscience & Biobehavioral Reviews* **30**, 730–748 (2006).
10. Courchesne, E. *et al.* Normal brain development and aging: quantitative analysis at in vivo MR imaging in healthy volunteers. *Radiology* **216**, 672–682 (2000).
11. McGinnis, S. M., Brickhouse, M., Pascual, B. & Dickerson, B. C. Age-related changes in the thickness of cortical zones in humans. *Brain topography* **24**, 279–291 (2011).
12. Tamnes, C. K. *et al.* Brain development and aging: overlapping and unique patterns of change. *Neuroimage* **68**, 63–74 (2013).
13. Douaud, G. *et al.* A common brain network links development, aging, and vulnerability to disease. *Proc. Natl. Acad. Sci. U.S.A.* **111**, 17648–17653 (2014).
14. Suzuki, H. *et al.* Associations of regional brain structural differences with aging, modifiable risk factors for dementia, and cognitive performance. *JAMA network open* **2**, e1917257–e1917257 (2019).
15. Fjell, A. M. *et al.* Development and aging of cortical thickness correspond to genetic organization patterns. *Proceedings of the National Academy of Sciences* **112**, 15462–15467 (2015).
16. Nyberg, L. *et al.* Individual differences in brain aging: heterogeneity in cortico-hippocampal but not caudate atrophy rates. *Cerebral Cortex* **33**, 5075–5081 (2023).
17. Alexander-Bloch, A., Giedd, J. N. & Bullmore, E. Imaging structural co-variance between human brain regions. *Nature Reviews Neuroscience* **14**, 322–336 (2013).
18. Whitwell, J. L. *et al.* Distinct anatomical subtypes of the behavioural variant of frontotemporal dementia: a cluster analysis study. *Brain* **132**, 2932–2946 (2009).
19. Levine, M. E. *et al.* An epigenetic biomarker of aging for lifespan and healthspan. *Aging (albany NY)* **10**, 573 (2018).
20. Demanelis, K. *et al.* Determinants of telomere length across human tissues. *Science* **369**, eaaz6876 (2020).

21. Foster, H. M. *et al.* The effect of socioeconomic deprivation on the association between an extended measurement of unhealthy lifestyle factors and health outcomes: a prospective analysis of the UK Biobank cohort. *The Lancet Public Health* **3**, e576–e585 (2018).
22. Townsend, P., Phillimore, P. & Beattie, A. *Health and Deprivation: Inequality and the North*. vol. 8 (Taylor & Francis, 2023).
23. Shi, R. *et al.* Structural neurodevelopment at the individual level - a life-course investigation using ABCD, IMAGEN and UK Biobank data. *medRxiv* 2023–09 (2023).
24. Smith, S. M. *et al.* An expanded set of genome-wide association studies of brain imaging phenotypes in UK Biobank. *Nature neuroscience* **24**, 737–745 (2021).
25. Grønborg, M. *et al.* Biomarker Discovery from Pancreatic Cancer Secretome Using a Differential Proteomic Approach* S. *Molecular & Cellular Proteomics* **5**, 157–171 (2006).
26. Liu, L., Watanabe, N., Akatsu, H. & Nishimura, M. Neuronal expression of ILEI/FAM3C and its reduction in Alzheimer's disease. *Neuroscience* **330**, 236–246 (2016).
27. Smith, S. M. *et al.* Brain aging comprises many modes of structural and functional change with distinct genetic and biophysical associations. *elife* **9**, e52677 (2020).
28. Estrada, K. *et al.* Genome-wide meta-analysis identifies 56 bone mineral density loci and reveals 14 loci associated with risk of fracture. *Nature genetics* **44**, 491–501 (2012).
29. Bohl, J., Brimer, N., Lyons, C. & Pol, S. B. V. The stardust family protein MPP7 forms a tripartite complex with LIN7 and DLG1 that regulates the stability and localization of DLG1 to cell junctions. *Journal of Biological Chemistry* **282**, 9392–9400 (2007).
30. Kaech, S. M., Whitfield, C. W. & Kim, S. K. The LIN-2/LIN-7/LIN-10 complex mediates basolateral membrane localization of the C. elegans EGF receptor LET-23 in vulval epithelial cells. *Cell* **94**, 761–771 (1998).
31. Lanktree, M. *et al.* Association study of brain-derived neurotrophic factor (BDNF) and LIN-7 homolog (LIN-7) genes with adult attention-deficit/hyperactivity disorder. *American Journal of Medical Genetics Part B: Neuropsychiatric Genetics* **147**, 945–951 (2008).
32. Habes, M. *et al.* Disentangling heterogeneity in Alzheimer's disease and related dementias using data-driven methods. *Biological psychiatry* **88**, 70–82 (2020).
33. Berg, D. *et al.* Prodromal Parkinson disease subtypes—key to understanding heterogeneity. *Nature Reviews Neurology* **17**, 349–361 (2021).
34. Ferreira, D., Nordberg, A. & Westman, E. Biological subtypes of Alzheimer disease: A systematic review and meta-analysis. *Neurology* **94**, 436–448 (2020).
35. Feczko, E. *et al.* The heterogeneity problem: approaches to identify psychiatric subtypes. *Trends in cognitive sciences* **23**, 584–601 (2019).
36. Poulakis, K. *et al.* Multi-cohort and longitudinal Bayesian clustering study of stage and subtype in Alzheimer's disease. *Nature communications* **13**, 4566 (2022).
37. Bogousslavsky, J., Miklossy, J., Deruaz, J.-P., Assal, G. & Regli, F. Lingual and fusiform gyri in visual processing: a clinico-pathologic study of superior altitudinal hemianopia. *Journal of Neurology, Neurosurgery & Psychiatry* **50**, 607–614 (1987).
38. Epstein, R., Harris, A., Stanley, D. & Kanwisher, N. The parahippocampal place area: recognition, navigation, or encoding? *Neuron* **23**, 115–125 (1999).
39. Mechelli, A., Humphreys, G. W., Mayall, K., Olson, A. & Price, C. J. Differential effects of word length and visual contrast in the fusiform and lingual gyri during. *Proceedings of the Royal Society of London. Series B: Biological Sciences* **267**, 1909–1913 (2000).

40. Chételat, G. *et al.* Using voxel-based morphometry to map the structural changes associated with rapid conversion in MCI: a longitudinal MRI study. *Neuroimage* **27**, 934–946 (2005).
41. Yao, Z. *et al.* Abnormal cortical networks in mild cognitive impairment and Alzheimer's disease. *PLoS computational biology* **6**, e1001006 (2010).
42. Christman, S. *et al.* Accelerated brain aging predicts impaired cognitive performance and greater disability in geriatric but not midlife adult depression. *Translational Psychiatry* **10**, 317 (2020).
43. Tian, Y. E. *et al.* Heterogeneous aging across multiple organ systems and prediction of chronic disease and mortality. *Nature Medicine* **29**, 1221–1231 (2023).
44. Aljondi, R., Szoeke, C., Steward, C., Yates, P. & Desmond, P. A decade of changes in brain volume and cognition. *Brain imaging and behavior* **13**, 554–563 (2019).
45. Raz, N. Aging of the brain and its impact on cognitive performance: Integration of structural and functional findings. (2000).
46. Honea, R., Crow, T. J., Passingham, D. & Mackay, C. E. Regional deficits in brain volume in schizophrenia: a meta-analysis of voxel-based morphometry studies. *American Journal of Psychiatry* **162**, 2233–2245 (2005).
47. Schultz, C. C. *et al.* Increased parahippocampal and lingual gyrification in first-episode schizophrenia. *Schizophrenia Research* **123**, 137–144 (2010).
48. Hoogman, M. *et al.* Brain imaging of the cortex in ADHD: a coordinated analysis of large-scale clinical and population-based samples. *American Journal of Psychiatry* **176**, 531–542 (2019).
49. Glahn, D. C. *et al.* Genetic basis of neurocognitive decline and reduced white-matter integrity in normal human brain aging. *Proceedings of the National Academy of Sciences* **110**, 19006–19011 (2013).
50. Brouwer, R. M. *et al.* Genetic variants associated with longitudinal changes in brain structure across the lifespan. *Nature neuroscience* **25**, 421–432 (2022).
51. Zheng, H.-F. *et al.* Whole-genome sequencing identifies EN1 as a determinant of bone density and fracture. *Nature* **526**, 112–117 (2015).
52. Ghafouri-Fard, S., Khoshbakht, T., Taheri, M. & Ghanbari, M. A concise review on the role of BDNF-AS in human disorders. *Biomedicine & Pharmacotherapy* **142**, 112051 (2021).
53. Association, W. M. & others. World Medical Association Declaration of Helsinki: ethical principles for medical research involving human subjects. *Jama* **310**, 2191–2194 (2013).
54. Desikan, R. S. *et al.* An automated labeling system for subdividing the human cerebral cortex on MRI scans into gyral based regions of interest. *Neuroimage* **31**, 968–980 (2006).
55. Fischl, B. *et al.* Whole brain segmentation: automated labeling of neuroanatomical structures in the human brain. *Neuron* **33**, 341–355 (2002).
56. Roweis, S. T. & Saul, L. K. Nonlinear dimensionality reduction by locally linear embedding. *science* **290**, 2323–2326 (2000).
57. Codd, V. *et al.* Polygenic basis and biomedical consequences of telomere length variation. *Nature genetics* **53**, 1425–1433 (2021).
58. Choi, S. W. & O'Reilly, P. F. PRSice-2: Polygenic Risk Score software for biobank-scale data. *Gigascience* **8**, giz082 (2019).
59. Thompson, D. J. *et al.* UK Biobank release and systematic evaluation of optimised polygenic risk scores for 53 diseases and quantitative traits. *MedRxiv* 2022–06 (2022).
60. Chang, C. C. *et al.* Second-generation PLINK: rising to the challenge of larger and richer datasets. *Gigascience* **4**, s13742-015 (2015).

642 61. Watanabe, K., Taskesen, E., Van Bochoven, A. & Posthuma, D. Functional mapping and annotation of
643 genetic associations with FUMA. *Nature communications* **8**, 1826 (2017).
644 62. Wang, K., Li, M. & Hakonarson, H. ANNOVAR: functional annotation of genetic variants from high-
645 throughput sequencing data. *Nucleic acids research* **38**, e164–e164 (2010).
646 63. Hawrylycz, M. J. *et al.* An anatomically comprehensive atlas of the adult human brain transcriptome.
647 *Nature* **489**, 391–399 (2012).
648 64. Markello, R. D. *et al.* Standardizing workflows in imaging transcriptomics with the abagen toolbox.
649 *elife* **10**, e72129 (2021).
650 65. Váša, F. *et al.* Adolescent Tuning of Association Cortex in Human Structural Brain Networks.
651 *Cerebral Cortex* **28**, 281–294 (2018).
652 66. Li, J. *et al.* Cortical structural differences in major depressive disorder correlate with cell type-specific
653 transcriptional signatures. *Nature communications* **12**, 1647 (2021).
654 67. Morgan, S. E. *et al.* Cortical patterning of abnormal morphometric similarity in psychosis is
655 associated with brain expression of schizophrenia-related genes. *Proceedings of the National Academy of*
656 *Sciences* **116**, 9604–9609 (2019).
657 68. Romero-Garcia, R. *et al.* Schizotypy-related magnetization of cortex in healthy adolescence is
658 colocated with expression of schizophrenia-related genes. *Biological psychiatry* **88**, 248–259 (2020).
659 69. Yu, G., Wang, L.-G., Han, Y. & He, Q.-Y. clusterProfiler: an R package for comparing biological
660 themes among gene clusters. *Omics: a journal of integrative biology* **16**, 284–287 (2012).

661

Acknowledgements

This research used the UK Biobank Resource under application number 19542. We thank all participants and researchers from the UK Biobank. We thank the IMAGEN Consortium for providing the discover data. This work received support from the following sources: the National Nature Science Foundation of China (No.82304241 [to X.L.]), National Key R&D Program of China (No.2019YFA0709502 [to J.F.], No.2018YFC1312904 [to J.F.]), Shanghai Municipal Science and Technology Major Project (No.2018SHZDZX01 [to J.F.], ZJ Lab [to J.F.], and Shanghai Center for Brain Science and Brain-Inspired Technology [to J.F.]), the 111 Project (No.B18015 [to J.F.]), the European Union-funded FP6 Integrated Project IMAGEN (Reinforcement-related behaviour in normal brain function and psychopathology) (LSHM-CT- 2007-037286 [to G.S.]), the Horizon 2020 funded ERC Advanced Grant 'STRATIFY' (Brain network based stratification of reinforcement-related disorders) (695313 [to G.S.]), Human Brain Project (HBP SGA 2, 785907, and HBP SGA 3, 945539 [to G.S.]), the Medical Research Council Grant 'c-VEDA' (Consortium on Vulnerability to Externalizing Disorders and Addictions) (MR/N000390/1 [to G.S.]), the National Institute of Health (NIH) (R01DA049238 [to G.S.], A decentralized macro and micro gene-by-environment interaction analysis of substance use behavior and its brain biomarkers), the National Institute for Health Research (NIHR) Biomedical Research Centre at South London and Maudsley NHS Foundation Trust and King's College London, the Bundesministeriumfür Bildung und Forschung (BMBF grants 01GS08152; 01EV0711 [to G.S.]; Forschungsnetz AERIAL 01EE1406A, 01EE1406B; Forschungsnetz IMAC-Mind 01GL1745B [to G.S.]), the Deutsche Forschungsgemeinschaft (DFG grants SM 80/7-2, SFB 940, TRR 265, NE 1383/14-1 [to G.S.]), the Medical Research Foundation and Medical Research Council (grants MR/R00465X/1 and MR/S020306/1 [to S.D.]), the National Institutes of Health (NIH) funded ENIGMA (grants 5U54EB020403-05 and 1R56AG058854-01 [to S.D.]), NSFC grant 82150710554 [to G.S.] and European Union funded project 'environMENTAL', grant no: 101057429 [to G.S.]. Further support was provided by grants from: - the ANR (ANR-12-SAMA-0004, AAPG2019 - GeBra [to J.-L.M.]), the Eranet Neuron (AF12-NEUR0008-01 - WM2NA; and ANR-18-NEUR00002-01 - ADORe [to J.-L.M.]), the Fondation de France (00081242 [to J.-L.M.]), the Fondation pour la Recherche Médicale (DPA20140629802 [to J.-L.M.]), the Mission Interministérielle de Lutte-contre-les-Drogues-et-les-Conduites-Addictives (MILDECA [to J.-L.M.]), the Assistance-Publique-Hôpitaux-de-Paris and INSERM (interface grant [to M.-L.P.M.]), Paris Sud University IDEX 2012 [to J.-L.M.], the Fondation de l'Avenir (grant AP-RM-17-013 [to M.-L.P.M.]), the Fédération pour la Recherche sur le Cerveau [to G.S.]; the National Institutes of Health, Science Foundation Ireland (16/ERCD/3797 [to R.W.]) and by NIH Consortium grant U54 EB020403 [to S.D.], supported by a cross-NIH alliance that funds Big Data to Knowledge Centres of Excellence. The funders had no role in study design, data collection and analysis, decision to publish or preparation of the manuscript.

Competing interests

Dr Banaschewski served in an advisory or consultancy role for eye level, Infectopharm, Lundbeck, Medice, Neurim Pharmaceuticals, Oberberg GmbH, Roche, and Takeda. He received conference support or speaker's fee by Janssen, Medice and Takeda. He received royalities from Hogrefe, Kohlhammer, CIP Medien, Oxford University Press; the present work is unrelated to these relationships. Dr Poustka served in an advisory or consultancy role for Roche and Viforpharm and received speaker's fee by Shire. She received royalties from Hogrefe, Kohlhammer and Schattauer. The present work is unrelated to the above grants and relationships. The other authors report no biomedical financial interests or potential conflicts of interest.

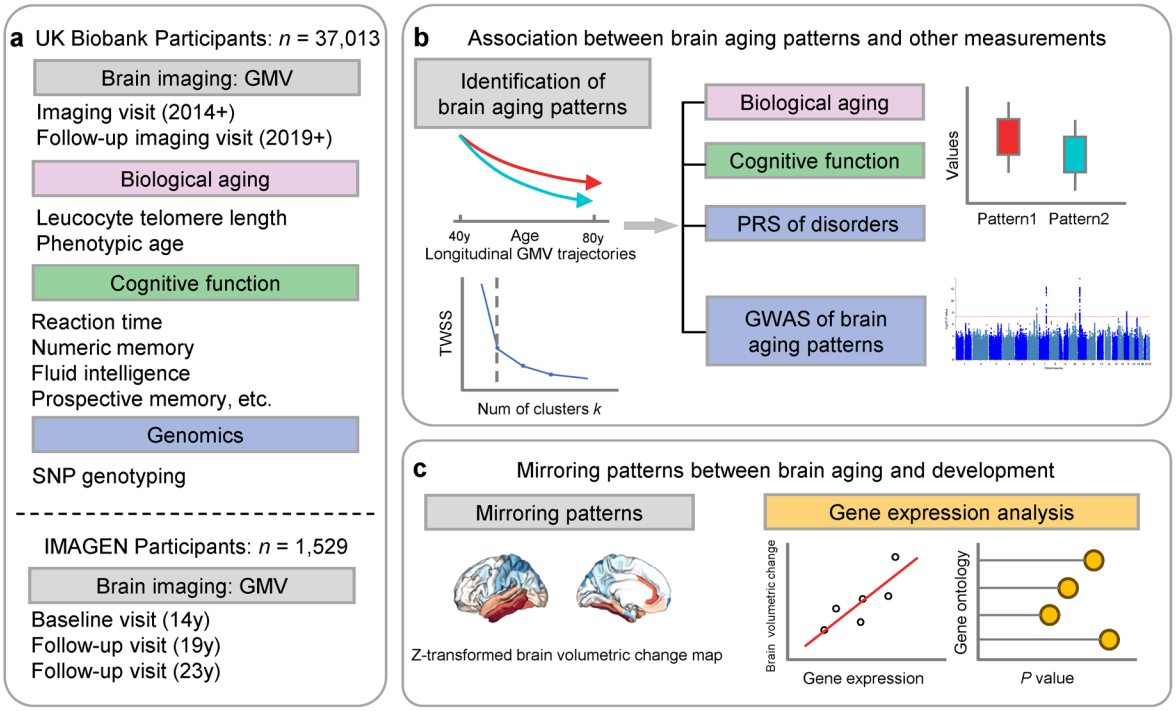

Figure 1. Overview of the study workflow. a, Population cohorts (UK Biobank and IMAGEN) and data sources (brain imaging, biological aging biomarkers, cognitive functions, genomic data) involved in this study. **b**, Brain aging patterns were identified using longitudinal trajectories of the whole brain GMV, which enabled the capturing of long-term and individualized variations compared to only use cross-sectional data, and associations between brain aging patterns and other measurements (biological aging, cognitive functions and PRS of major neuropsychiatric disorders) were investigated. c, Mirroring patterns between brain aging and brain development was investigated using z-transformed brain volumetric change map and gene expression analysis.

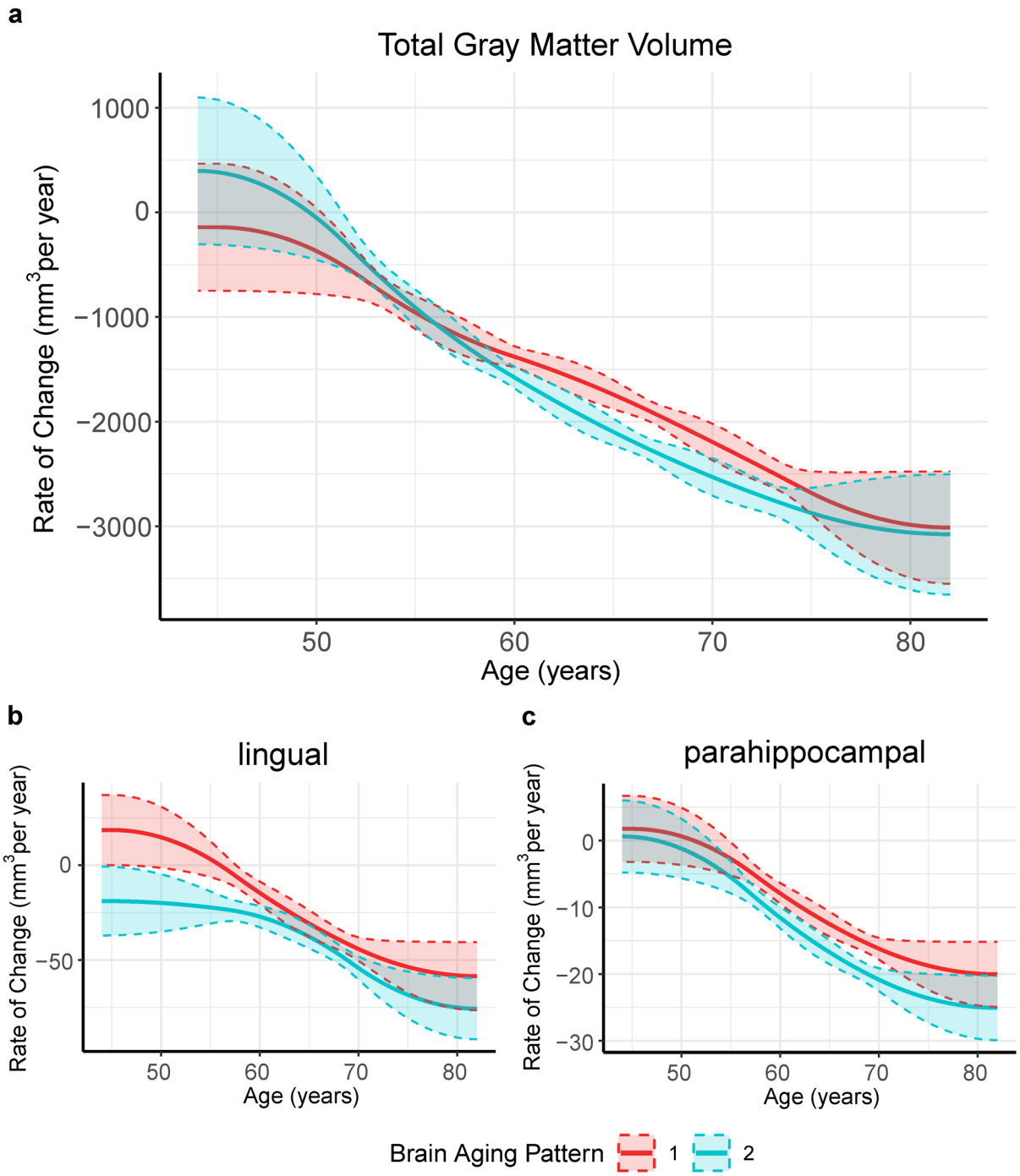

Figure 2. Global (a) and selected regional (b, c) cortical gray matter volume rate of change among participants with brain aging patterns 1 (red) and 2 (blue). Rates of volumetric change for total gray matter and each ROI were estimated using GAMM, which incorporates both cross-sectional between-subject variation and longitudinal within-subject variation from 40,921 observations and 37,013 participants. Covariates include sex, assessment center, handedness, ethnic, and ICV. Shaded areas around the fit line denotes 95% CI.

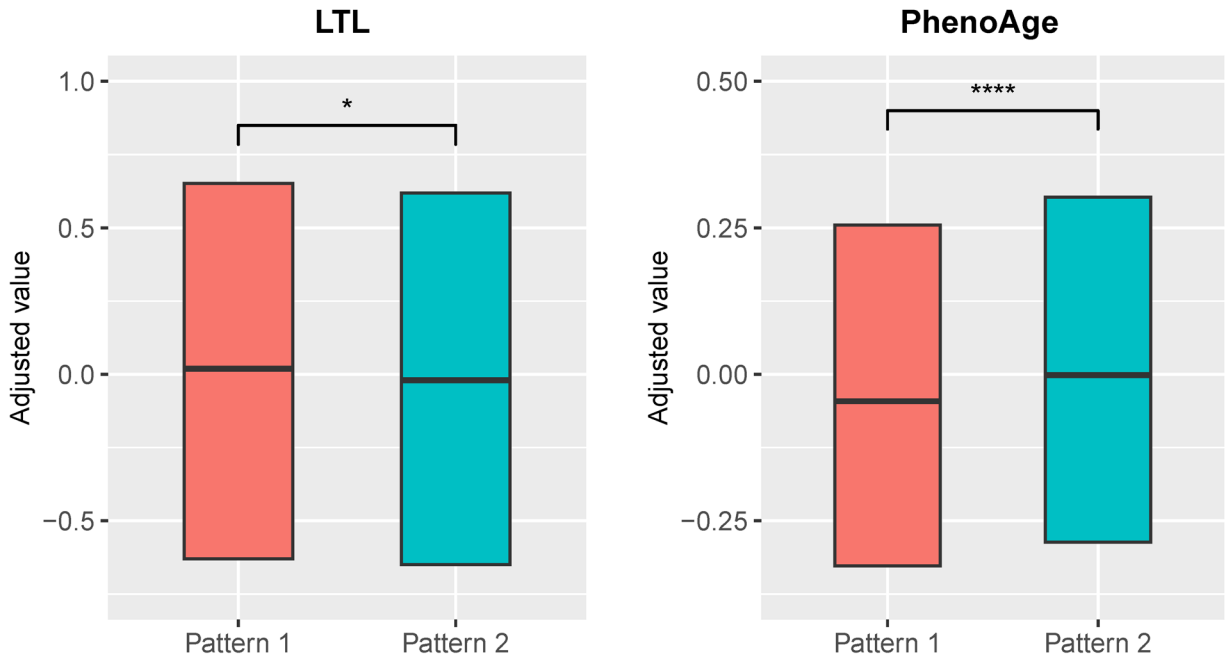

Figure 3. Distributions of biological aging biomarkers (leucocyte telomere length (LTL) and PhenoAge) among participants with brain aging patterns 1 and 2. Boxes represent the interquartile range (IQR), lines within the boxes indicate the median. Two-sided P values were obtained by comparing LTL or PhenoAge[19] between brain aging patterns using unadjusted multivariate linear regression models. Results remained significant when adjusting for sex, age, ethnic, BMI, smoking status and alcohol intake frequency in the LTL model[20] and sex, age, ethnic, BMI, smoking status, alcohol frequency and education years in PhenoAge model. Stars indicate statistical significance after Bonferroni correction. ****: $p <= 0.0001$, *: $p <= 0.05$.

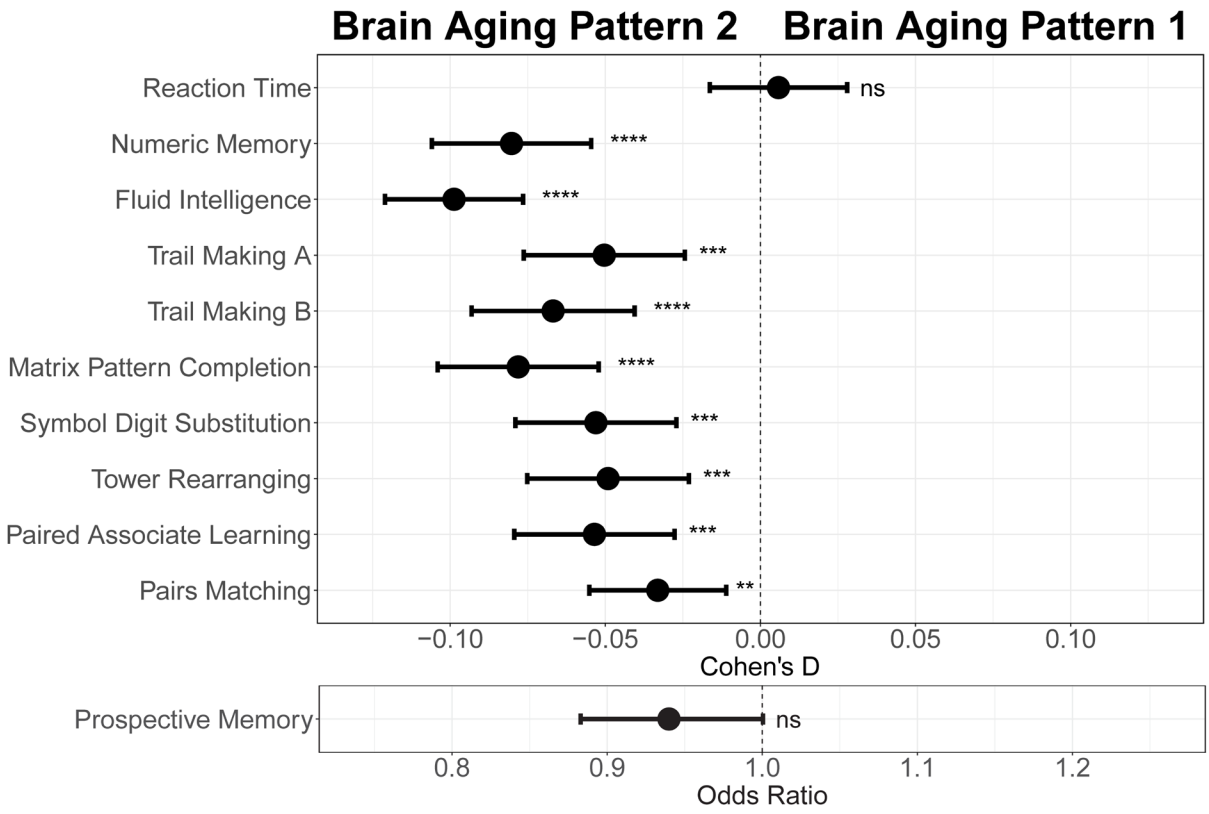

Figure 4. Effect size (Cohen's D or odds ratio) for comparing the cognitive functions between participants with brain aging patterns 1 and 2. Results were adjusted such that negative Cohen's D and Odds Ratio less than 1 indicate worse cognitive performances in brain aging pattern 2 compared to pattern 1. Width of the lines extending from the center point represent 95% confidence interval. Two-sided P values were obtained using both unadjusted and adjusted (for sex, age, and TDI, education and income) multivariate regression models. Stars indicate statistical significance after FDR correction for 11 comparisons. ****: p <= 0.0001, ***: p <= 0.001, **: p <= 0.01, ns: p > 0.05.

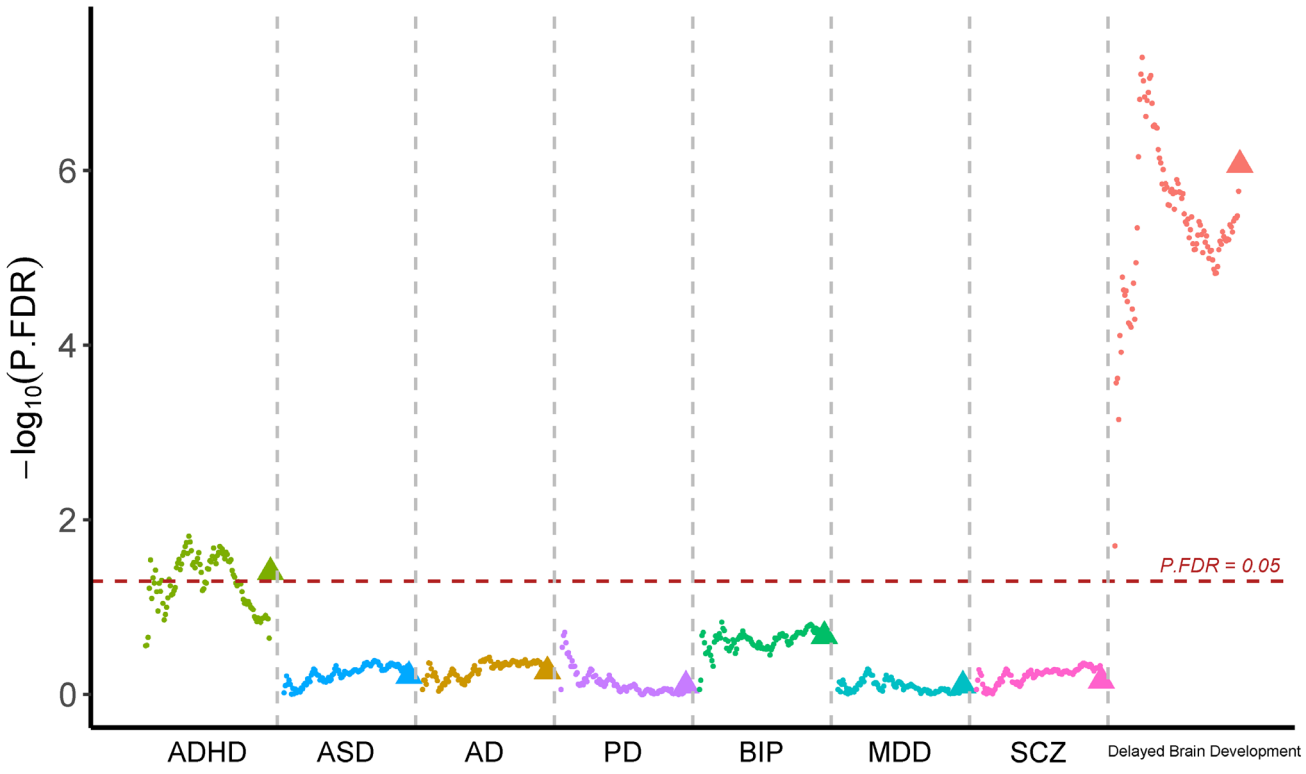

Figure 5. Participants with accelerated brain aging (brain aging pattern 2) had significantly increased genetic liability to ADHD and delayed brain development. Polygenic risk score (PRS) for ADHD, ASD, AD, PD, BIP, MDD, SCZ and delayed brain development (unpublished GWAS) were calculated at different p-value thresholds from 0.005 to 0.5 at an interval of 0.005. Vertical axis represents negative logarithm of P values comparing PRS in brain aging pattern 2 relative to pattern 1. Red horizontal dashed line indicates FDR corrected P value of 0.05. Colors represent traits and dots within the same color represent different p value thresholds. The trigonometric symbol indicates the average PRS across all p-value thresholds for the same trait.

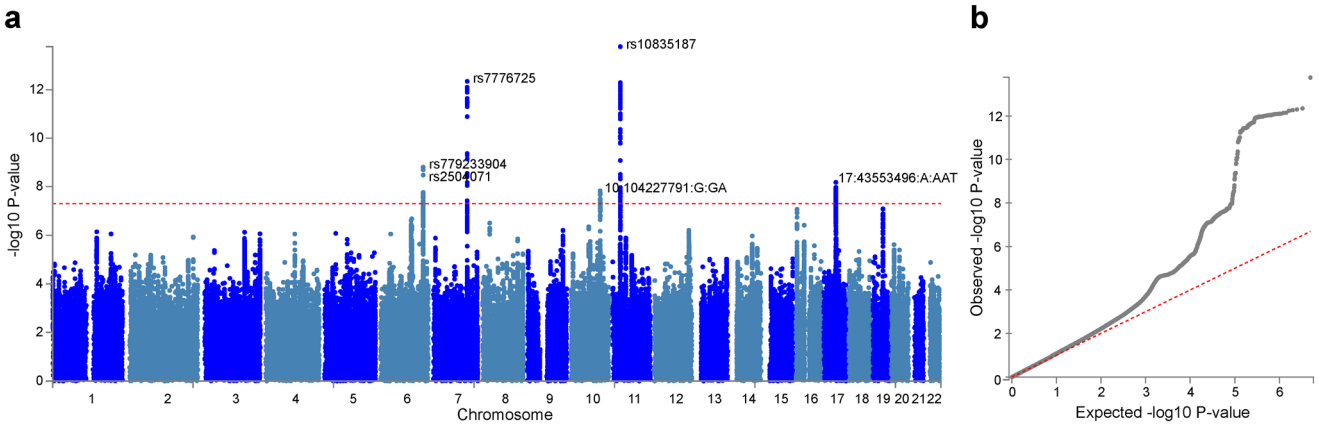

Figure 6. Genome-wide association study (GWAS) identified 6 independent SNPs associated with accelerated brain aging. Total GMV at 60 years old was estimated for each participant using mixed effect models allowing for individualized baseline GMV and GMV change rate, and was used as the phenotype in the GWAS. **a**, At genome-wide significance level ($P = 5 \times 10^{-8}$, red dashed line), rs10835187 and rs7776725 loci were identified to be associated with accelerated brain aging. **b**, Quantile–quantile plot showed that the most significant P values deviate from the null, suggesting that results are not unduly inflated.

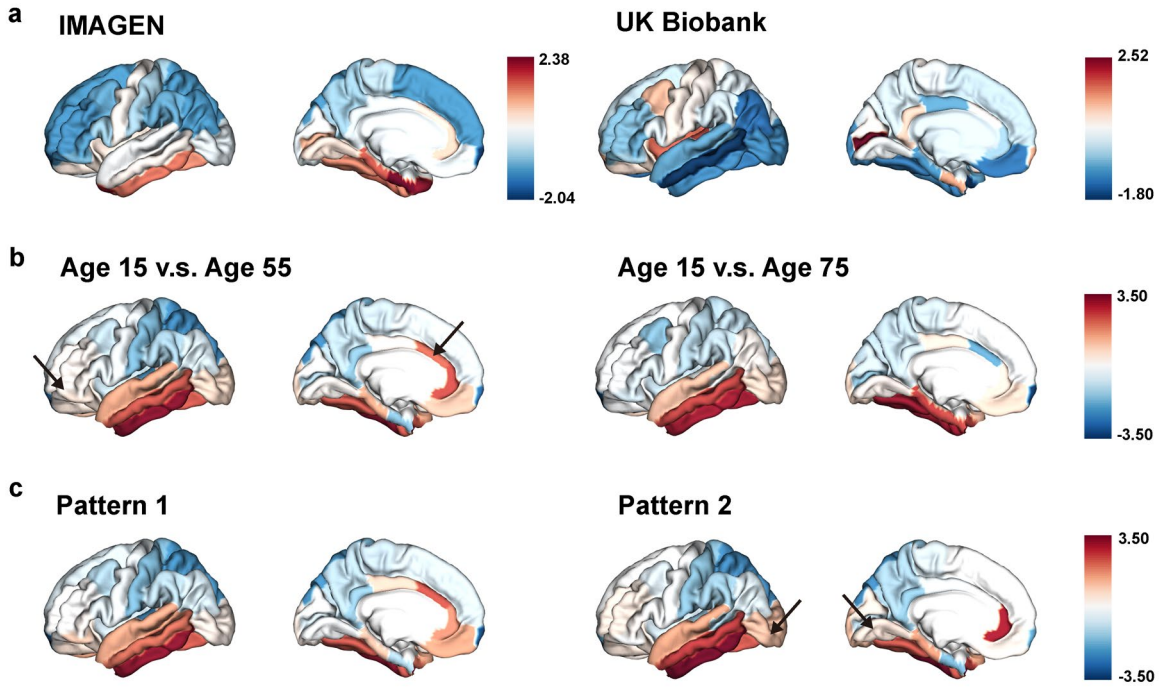

Figure 7. The "last in, first out" mirroring patterns between brain development and brain aging. a, The annual percentage volume change (APC) was calculated for each ROI and standardized across the whole brain in adolescents (IMAGEN, left) and mid-to-late aged adults (UK Biobank, right), respectively. For adolescents, ROIs of in red indicate delayed structural brain development, while for mid-to-late aged adults, ROIs in blue indicate accelerated structural brain aging. **b**, Estimated APC in brain development versus early aging (55 years old, left), and versus late aging (75 years old, right). ROIs in red indicate faster GMV decrease during brain aging and slower GMV decrease during brain development, i.e., stronger mirroring effects between brain development and brain aging. **c**, Mirroring patterns between brain development and brain aging were more manifested in participants with accelerated aging (brain aging pattern 2). The arrows point to ROIs with more pronounced mirroring patterns in each subfigure.

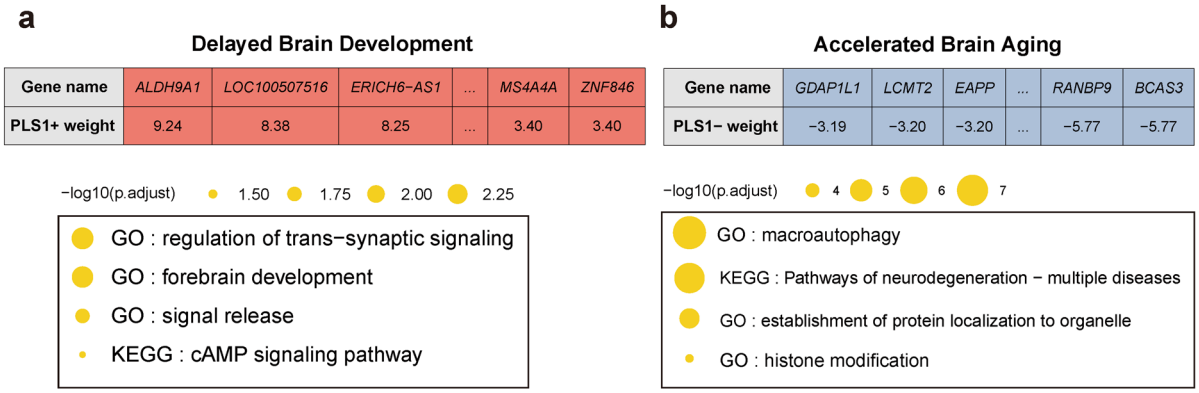

Figure 8. Functional enrichment of gene transcripts significantly associated with delayed brain development and accelerated brain aging. a, 990 genes were spatially correlated with the first PLS component of delayed structural brain development, and were enriched for trans-synaptic signal regulation, forebrain development, signal release and cAMP signaling pathway. **b**, 2,293 genes were spatially correlated the first PLS component of accelerated structural brain aging, and were enriched for macroautophagy, pathways of neurodegeneration, establishment of protein localization to organelle and histone modification. Size of the circle represents number of genes in each term and P values were corrected using FDR for multiple comparisons.